AUTOMATED ANTARCTIC ICE EDGE DETECTION USING NSCAT DATA

Quinn P. Remund and David G. Long
Brigham Young University, MERS Laboratory
459 CB, Provo, UT 84602
801-378-4884, FAX: 801-378-6586 remundq@nscat.ee.byu.edu

Abstract— Polar sea ice plays an important role in the global climate and other geophysical processes. Although spaceborne scatterometers such as NSCAT have low inherent spatial resolution, resolution enhancement techniques can be utilized to make NSCAT data useful for monitoring sea ice extent in the Antarctic. Dual polarization radar measurements are $\mathcal{A}$ and $\mathcal{B}$ values are used in a linear discrimination analysis to identify sea ice and ocean pixels in composite images. Ice edge detection noise reduction is performed through region growing and erosion/dilation techniques. The algorithm is applied to actual NSCAT data. The resulting edge closely matches the NSIDC SSM/I derived 50% ice concentration edge.

INTRODUCTION

Historically, space-borne scatterometers have been employed primarily in atmospheric and oceanic studies. Rapid repeat coverage makes these instruments valuable in these applications. The low nominal spatial resolution inherent to scatterometers is acceptable for studying such large scale phenomenon. Spaceborne scatterometers have also been used to study non-ocean surface parameters (e.g. [1] [2]). However, for land and ice studies, the low resolution can limit the utility of this data.

The Scatterometer Image Reconstruction with Filter (SIRF) algorithm was developed [3] to enhance scatterometer image resolution by combining data from multiple passes of the satellite. It uses multiple σ^o values to increase the effective resolution of the data. Over a limited incidence angle range of [20°,55°], σ^o (in dB) is a approximately a linear function of θ,

$$\sigma^o(\theta) = \mathcal{A} + \mathcal{B}(\theta - 40^\circ)$$

where $\mathcal{A}$ and $\mathcal{B}$ are functions of surface characteristics, azimuth angle, and polarization. $\mathcal{A}$ is the σ^o value at 40° incidence and $\mathcal{B}$ describes the dependence of σ^o on θ. $\mathcal{A}$ and $\mathcal{B}$ provide valuable information about surface parameters. 40 deg was chosen as a mid-swath value, but any interior swath angle can be used.

Polar sea ice is a critical input to global climate and geophysical models. It acts as an insulating layer between the warmer ocean and cooler atmosphere and can radically change the albedo of the Earth's surface. Hence, monitoring the extent of polar sea ice is of great interest to the remote sensing community. An automated algorithm for detecting the polar sea ice edge from NSCAT data has been developed and shown to estimate the actual Antarctic ice edge with a high degree of accuracy. This paper describes the development and implementation of this algorithm.

ANTARCTIC NSCAT DATA

The NASA Scatterometer (NSCAT) launched in August of 1996 is a real aperture dual polarization Ku-band radar scatterometer designed to measure the normalized radar backscatter coefficient (σ^o) of the earth's surface. The two polarization $\mathcal{A}$ and $\mathcal{B}$ values provide four parameters that can be used to detect polar sea ice. Each of these parameters contains different information about the surface that may be useful in the discriminant analysis. This section examines the statistical properties of these variables to determine which combination provides the best basis for discrimination between ice and open ocean.

The $\mathcal{A}$V/$\mathcal{A}$H ratio is useful in determining the amount of volume versus surface scattering. In log space, this is equivalent to taking the difference between the V and H components. For smooth, conductive surfaces such as sea water, different reflection coefficients exist for vertically and horizontally polarized incident waves. In general, vertically polarized waves will reflect more than their horizontal counterparts. Thus, the $\mathcal{A}$V/$\mathcal{A}$H ratio will be positive. In volume scattering situations from dielectric surfaces with randomly oriented scatterers, such as ice with low water content, multiple reflections of the incident radiation tends to depolarize it. As a result, vertical and horizontal waves are scattered similarly and the $\mathcal{A}$V/$\mathcal{A}$H ratio is very close to one. Thus the $\mathcal{A}$V/$\mathcal{A}$H ratio is useful in discriminating between surfaces that display these scattering mechanisms.

According to the previous discussion, the ocean will generally have high $\mathcal{A}$V/$\mathcal{A}$H ratio values while sea ice (with low water content) will have low values. In actual $\mathcal{A}$V/$\mathcal{A}$H images, this is generally the case. However, in high wind conditions some ocean areas do exhibit low $\mathcal{A}$V/$\mathcal{A}$H ratios. The winds induce roughness on the ocean surface which depolarizes the scattering and drives the $\mathcal{A}$V/$\mathcal{A}$H ratio down. To minimize the effects of this error, the $\mathcal{B}$ parameters are also used to classify the data.

$\mathcal{B}$ Values

$\mathcal{B}$ values represent the incidence angle dependence of σ^o. Ice tends to be more isotropic than open water and has

0-7803-3836-7/97/$10.00

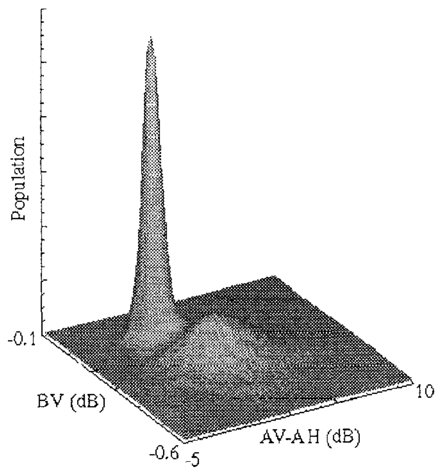

Figure 1: *Two dimensional distribution of $\mathcal{A}V/\mathcal{A}H$ values vs. $\mathcal{B}V$ values. The two modes correspond with ice and ocean pixels.*

less incidence angle dependence. Ocean σ^o is strongly dependent on incidence angle with the low incidence angles exhibiting higher σ^o. A strong correlation exists between $\mathcal{B}$V and $\mathcal{B}$H. Noting that $\mathcal{B}$V values are less noisy than $\mathcal{B}$H due to the greater number of vertical polarization measuremnts, $\mathcal{B}$V was chosen for the discriminant analysis in this study.

Multi-Parameter Analysis

The $\mathcal{A}V/\mathcal{A}H$ ratio is combined with the $\mathcal{B}$V value for each pixel in a resolution enhanced image for classification. For all non-land pixels a $\mathcal{A}V/\mathcal{A}H$ ratio vs. $\mathcal{B}$V two dimensional distribution is plotted in Figure 1. The two modes of the distribution correspond with sea ice and ocean pixels. Figure 2 illustrates a contour plot of the $\mathcal{A}V/\mathcal{A}H$ ratio vs. $\mathcal{B}$ V distribution. The linear discrimination line is also plotted and is addressed in a following section. The contour level corresponds to the point at which the separate distributions begin to overlap and was used to set the linear threshold value.

ALGORITHM DESCRIPTION

Several steps are required to implement the actual ice edge detection. Initial steps (1-2) prepare the data and perform the linear discrimination. Following steps (3-4) are taken to reduce the effects of noise caused by misclassification. The general steps are as follows:

1. Generate the $\mathcal{A}V/\mathcal{A}H$ ratio and $\mathcal{B}V$ images.
2. Produce binary threshold image through linear discriminant analysis.
3. Use region growing techniques to eliminate isolated patches of noise.
4. Use erosion and dilation techniques to reduce edge noise.
5. Apply the mask to the desired image.

Once SIRF images are generated from 6 days of NSCAT data, the difference is taken of the $\mathcal{A}$V and $\mathcal{A}$H images in log space to create a $\mathcal{A}V/\mathcal{A}H$ ratio image. A median filter is then applied to reduce speckle in the image. The median filter was chosen since it is an edge preserving operation.

Linear Discrimination

The linear discrimination function is given by

$$\mathcal{B}V = 0.0295(\mathcal{A}V/\mathcal{A}H) - 0.23$$

where $\mathcal{B}$V and $\mathcal{A}V/\mathcal{A}H$ are in dB. This line is plotted over the contour plot in Figure 2. For each pixel in question, the $\mathcal{A}V/\mathcal{A}H$ value is used in this equation to derive a $\mathcal{B}$V threshold value. If the observed $\mathcal{B}$V value is greater than this threshold, the pixel is classified as ice, otherwise the pixel is considered ocean. This binary decision is performed for each pixel in the image.

Noise Removal

The lincar discrimination portion of thc algorithm results in a binary image illustrating the location of sea ice and ocean regions. High winds over the ocean can cause ocean pixels to be misclassified as ice for reasons previously addressed. This noise is manifested in the binary image as

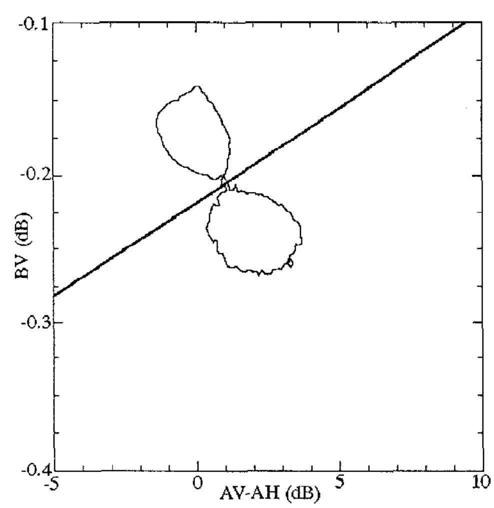

Figure 2: *Contour plot of the distribution at the point where the modes intersect. The decision boundary line is plotted as well.*

patches of ocean that have been classified as sea ice and patches of ice that were classified as ocean. Some of these are small isolated regions in the ocean area while others occur on or near the actual ice edge and are thus connected to the large ice region of the image. Each of these is handled separately in the noise removal step.

Region growing techniques are used to eliminate the isolated misclassification patches in the ocean. The region growing algorithm starts with a small region known to be within the ice area. It then expands this region within the ice area of the binary threshold image. The region continues to grow until it gets to the outer edge of the ice region. This eliminates all the patches of pixels misclassified as ice in the ocean. The region growing algorithm is then inverted to grow from the outer edge of the image inward until it reaches the binary threshold edge. This eliminates all the patches of pixels misclassified as ocean in the ice.

Once the region growing is complete, some residual noise exists on the edge itself as high spatial frequency edge characteristics and as small lobes attached by only a few pixels to the main body of ice. To remove this, image erosion and dilation techniques [4] are used. Two erosion iterations separate the smaller misclassified lobes from the main body. Region growing is then performed again to eliminate these separated lobes. To restore the edge (a low pass filtered version), two iterations of image dilation are performed.

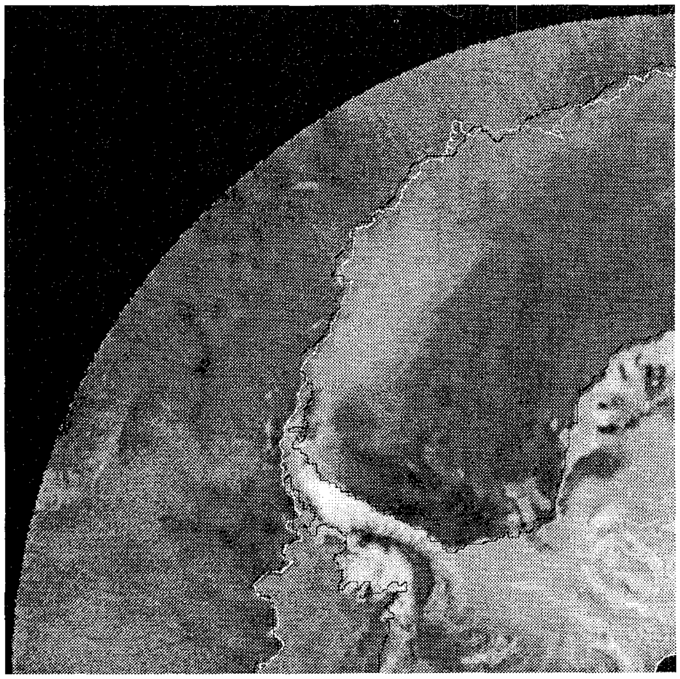

Figure 3: *NSCAT SIRF enhanced $\mathcal{A}$ value vertical polarization image of a portion of Antarctica with ice edges plotted. The white edge was derived from the NSCAT algorithm while the black edge corresponds to the NSIDC SSM/I 50% ice edge.*

The result is a binary image depicting the location of sea ice and ocean. This is then used to mask the original resolution enhanced images.

RESULTS

The algorithm was implemented using SIRF resolution enhanced Antarctic images for the time period 1996 JD 276-281. Figure 3 shows a region of Antarctica with an ice edge derived from this algorithm plotted over the top. Another ice edge is plotted in the image that was created from thresholded NSIDC SSM/I ice concentration images. This particular edge corresponds with a 50% ice concentration. This level produced an edge had the highest correlation with the NSCAT derived ice edge.

CONCLUSIONS

NSCAT dual polarization Ku-band data in concert with the SIRF resolution enhancement algorithm can be used to effectively determine sea ice extent in the Antarctic. Linear discrimination analysis differentiates between ice and ocean pixels with a high degree of accuracy. Region growing and erosion/dilation procedures are effective in minimizing the effects of residual misclassified pixels. The resulting ice edge correlates very well with the NSIDC SSM/I derived 50% ice concentration edge.

REFERENCES

[1] D. Long and M. Drinkwater, "Greenland Ice-Sheet Surface Properties Observed by the Seasat-A Scatterometer at Enhanced Resolution", *J. of Glaciology*, vol. 40, no. 135, pp. 213–230, 1994.

[2] A. R. Hosseinmostafa, V. I. Lytle, K. C. Jezek, S. P. Gogineni, S. F. Ackley, and R. K. Moore, "Comparison of Radar Backscatter from Antarctic and Arctic Sea Ice", *J. of Electromagnetic Waves and Applications*, vol. 9, no. 3, pp. 421–438, 1995.

[3] D. Long, P. Hardin, and P. Whiting, "Resolution Enhancement of Spaceborne Scatterometer Data", *IEEE Trans. on Geosci. and Rem. Sens.*, vol. 31, pp. 700–715, 1993.

[4] J.C. Rush, *The Image Processing Handbook, 2nd Ed.*, CRC Press, Boca Raton, FL, 1995.

ACKNOWLEDGMENTS

SSM/I data provided by the EOS Distributed Active Archive Center (DAAC) at the National Snow and Ice Data Center. NSCAT data provided by PO.DAAC at the Jet Propulsion Laboratory.